Charge transfer between carbon nanotubes and sulfuric acid as determined by Raman spectroscopy

Pascal Puech,[1,*] Tao Hu,[2] Andrei Sapelkin,[3] Iann Gerber,[2] Victoria Tishkova,[1] Ekaterina Pavlenko,[1] Benjamin Levine,[1] Emmanuel Flahaut,[4] and Wolfgang Bacsa[1]

[1]*CEMES, UPR 8011, CNRS-Université de Toulouse, 29, rue Jeanne Marvig, BP 94347, 31055 Toulouse, France*
[2]*Université de Toulouse, INSA-CNRS-UPS, LPCNO, 135 Avenue de Rangueil, 31077 Toulouse, France*
[3]*Department of Physics, Queen Mary University of London, Mile End Road, E1 4 NS London, United Kingdom*
[4]*Université de Toulouse, Institut Carnot CIRIMAT, Université Paul-Sabatier, 118 route de Narbonne, 31062 Toulouse, France*

The spontaneous interaction between sulfuric acid and carbon nanotubes is studied using Raman spectroscopy. We are able to determine the charge transfer without any additional parameter using the spectral signature of inner and outer walls of double-wall carbon nanotubes. While for the outer wall both the lattice contraction and the nonadiabatic effects contribute to the phonon shift, only the lattice contraction contributes for the inner nanotube. For the outer nanotube, we are able to separate these two contributions of the Raman G-band shift as a function of the charge transfer. We have carried out density functional theory calculations on graphene to see how different chemical species (HSO_4^-, H_2SO_4, H^+) affect the electronic band structure and electron-phonon coupling. The Raman G-band shift for the outer nanotube, $\Delta\omega$, as a function of hole charge transfer per carbon atom, f_C, is found to be $\Delta\omega\ (\mathrm{cm}^{-1}) = (350 \pm 20) f_C + (101 \pm 8)\sqrt{f_C}$.

I. INTRODUCTION

Electrical properties of carbon nanotubes (CNT) are particularly attractive when incorporating them into polymers for shielding applications or making electrical wires.[1] The efficient dispersion of CNTs in strong acids and the formation of a nematic phase has been used to fabricate fibers with aligned CNTs.[2] Raman spectroscopy is an effective and noninvasive characterization tool to monitor true thermodynamic solutions.[3] The Raman shift of the G^+ band is an excellent indicator of the hole charge transfer per carbon atom f_C. Sumanasekera *et al*. have determined a value of 320 f_C (cm^{-1}) for the Raman shift for the electrochemically doped single-wall CNTs (SW) using sulfuric acid solutions.[4] However, in order to analyze the Raman shift of nanotubes in an acid solution, it is important to be able to separate the effect of lattice contraction (and hence of the strain) due to charge transfer and the effect of the electron-phonon coupling due to Fermi level shift. We use here double-wall CNTs (DW) to separate lattice contraction from electron-phonon coupling deduced G-band shifts, which is crucial for the understanding of electrochemical doping of nanotubes.[3,5]

Theoretically, one can take benefit of the similarity between noncovalent doping of large-diameter SW and graphene models.[6] We also use graphite intercalated compounds (GICs) results for comparison. When intercalating GIC with H_2SO_4, the charge transfer coefficient changes by a factor 2.6 between stage 1 (a graphene monolayer surrounded on both sides with sulfuric acid) and stage 2 (a graphene bilayer surrounded by sulfuric acid), corresponding, respectively, to 460 f_C and 1200 f_C in cm^{-1}[7]. The absolute phonon shift for stage 1 (51 cm^{-1}) divided by the charge transfer ($f_C = 1/28$) yields 1430 f_C in cm^{-1}. Hydrogen is removed during the intercalation process.

Lazzeri and Mauri[8] have computed electron-phonon coupling in graphene using first-principles calculations to separate out the strain contribution. A hardening of the phonons is predicted due to nonadiabaticity attributed to movement of the Fermi level near the Dirac point. The total phonon shift can be separated into a contribution due to the lattice contraction (strain) $\Delta\omega_s$ and a contribution due to the nonadiabatic effects (dynamical) labeled $\Delta\omega_d$ given by

$$\Delta\omega = \Delta\omega_s + \Delta\omega_d,$$

with

$$\Delta\omega_s\ (\mathrm{cm}^{-1}) = 350 f_C,$$

obtained from Fig. 1 of Ref. 8, and by converting the Fermi level shift in hole charge transfer per carbon atom in the algebraic Eq. (13) of Ref. 8:

$$\Delta\omega_d\ (\mathrm{cm}^{-1}) = 216\sqrt{f_C} + 1.74 \ln\left(\left|\frac{6.04\sqrt{f_C} - 0.096}{6.04\sqrt{f_C} + 0.096}\right|\right).$$

For large f_C, the last term can be ignored (5% of modification of $\Delta\omega_d$ for $f_C = 0.005$). For the conversion, we use $f_C = -0.002\,65\,\sigma$, where σ is the surface electron concentration in 10^{-13} cm^{-1}.

It is important to keep in mind that there is a fundamental difference between chemical doping, where new electronic states are introduced, and a gate-induced doping in a solid-state device, where the position of the Fermi level is modified by the gate voltage while the electronic band structure is left intact. A nonadiabatic effect can change the phonon energy by up to 30% in GIC, which can be considered as a limiting case of doped graphene with intercalants.[9] However, the nonadiabatic effect can be removed by the modification of the electronic band structure. GIC with sulfuric acid is more complicated to calculate because the dissociation of the species has to be fully taken into account. While bulk graphite is inert in sulfuric acid, a spontaneous interaction occurs when CNTs are exposed to sulfuric acid.[4] Protonation and formation of layers around the nanotubes has been experimentally observed.[10–14] So far the Raman shift due to charge transfer has been deduced through electrochemical measurements using 320 f_C in cm^{-1} (Ref. 4). This conversion factor for charge transfer value is not in accord

with the phonon shifts observed in GIC. While the variation of the wave-number shift in the electrochemical measurements is linear with f_C, Lazzeri and Mauri[8] shows that apart of the linear strain dependence, an additional nonadiabatic term exists which is proportional to $\sqrt{f_C}$. The interaction of charged species with the nanotubes is complex and so far no attempt has been made to independently link the observed phonon wave-number shift with charge transfer taking into account the strain-induced effects. The modification of the electron-phonon coupling by perturbing the band structure near the Fermi level needs to be taken into account. The accurate value of the spontaneous wave-number shift due to this effect is important when optimizing processes when working with large amounts of nanocarbons.

The Raman spectrum of pristine SW is composed of a G^+ mode (1592 cm^{-1}) and a less intense G^- mode. The position of the G^- mode is diameter dependent and also depends on whether the nanotube is metallic or semiconducting.[15] For DW, there are two main contributions attributed to the two G^+ modes that are located at 1592 cm^{-1} for the outer nanotube and 1581 cm^{-1} for the inner nanotube. The G^- modes are weaker in intensity and are located at lower wave numbers.[16] The G^- band has a complex behavior.[17] The G^+ bands overlap at normal pressure and split with increasing pressure.[18]

Using SW, the phonon shift induced by doping is due to both lattice contraction and electron-phonon coupling. Hence, a calibration is necessary to determine the contribution of both effects. DWs are ideal for this purpose. Their inner nanotube can be taken as a strain indicator while their outer nanotube is affected by charge transfer that contracts bonds and modifies electron-phonon coupling. As the strain is linear with the charge transfer,[8,19] we can determine from the inner nanotube the strain of the outer nanotube and subsequently the intrinsic charge transfer. We use temperature- and pressure-dependent measurements as a function of sulfuric acid concentration to verify our assessments. With GIC, HSO_4^- is the main species in interaction with the graphene sheet.[7] Undissociated H_2SO_4 has been proposed as dopant.[20] Moreover, for CNTs, protonation has been observed experimentally.[10–12] To understand which species is really a dopant and thus what is the associated modification of the electronic band structure, we have conducted density functional theory (DFT) calculations with periodic boundary conditions using H_2SO_4, H, and HSO_4. These are the three major molecular species in pure sulfuric acid. We compare our results to the literature and explain why, for CNTs, the wave-number shift versus the charge transfer is composed of a part due to lattice contraction and a part due to nonadiabatic effects.

II. EXPERIMENTAL AND COMPUTATIONAL INFORMATION

A. Samples and experiments

Purified SW material was purchased from Nanocarblab (electric arc method, diameter range: 1.2–1.6 nm). DWs were synthesized using catalytical chemical vapor deposition.[21] The outer diameter ranges from 1.3 to 2.2 nm. One milligram of each material was immersed in 1 mL of sulfuric acid at 98% (or 120%) purchased from Aldrich Company. The high-pressure Raman measurements were performed in a diamond anvil cell (DAC) using a Renishaw spectrometer. The hydrostatic pressure was measured using the R-line emission of a small chip of ruby placed in the DAC. This allowed calibration[22] of the pressure to within ± 0.1 GPa. We observed a clear double peak from the ruby emission at all pressures. The solution with nanotubes has been injected in a hole which was drilled in the steel gasket. After closing the cell, a visual checking ensured that the material was present and the phonon spectrum was used to detect doping level. Sulfuric acid reacts to some degree with steel and absorbs water humidity, leading to a reduction of the overall doping. To reduce this effect we have dried the gasket before loading. The laser power incident on the sample was estimated to be 12 mW (spot size around 3 μm with an objective $\times 20$). The wavelength used was 632.8 nm.

Temperature-dependent measurements were conducted on a droplet of sulfuric acid with nanotubes between two glass slides using a T64000 Jobin-Yvon Horiba spectrometer. As the partial pressure is low and the temperature of vaporization (dissociation) high (340 °C), we dried the cryostat by heating it and used nitrogen atmosphere to avoid water adsorption during the experiment. A red (647 nm) and a blue (476 nm) excitation wavelengths were used. The solution was sensitive to laser power. The spectra changed above 0.5 mW with an objective lens $\times 50$ and a new mode appeared at around 1570 cm^{-1}, which made accurate fitting difficult.

To estimate the uncertainties, we considered both the standard deviation and the inherent error of all reported values.[23]

B. Calculations

DFT calculations were performed on a (7×7) primitive cell of graphene, containing 98 C atoms, using the Vienna *ab initio* simulation package VASP.[24–27] A coverage value of one molecule per 98 carbon atoms was used to study doping effects. The code uses the full-potential projector augmented wave (PAW) framework.[28,29] Exchange-correlation effects have been approximated using the PBE functional[30] and applied in spin-polarized calculations. In addition, we have tested the so-called vdW-DF[31] as implemented in VASP.[32] A kinetic energy cutoff of 400 eV was found to be sufficient to achieve a total-energy convergence within several meV considering a k-point sampling with a $(3 \times 3 \times 1)$ grid. Charge analysis was performed using Bader formalism.[33–35]

III. RESULTS

When CNTs are immersed in superacids, a spontaneous interaction takes place.[3] Before considering the measured Raman shift in greater detail, we discuss the spontaneous interaction of sulfuric acid with nanotubes as a function of temperature and pressure.

A. Temperature effect: SW and DW

Figure 1 shows the Raman spectra of SW and DW in concentrated solution at room temperature and by increasing the temperature from 0 °C to 50 °C by steps of 10 °C using excitation wavelength of 647 nm for SW and 478 nm for DW.

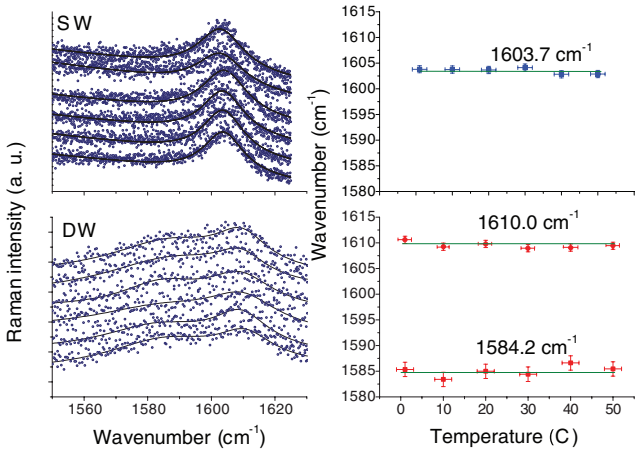

FIG. 1. (Color online) Raman spectra of SW and DW in concentrated sulfuric acid as a function of temperature. Each spectra has been recorded by increasing the temperature by 10 K. Wavelengths of the laser are 647 nm for SW and 478 nm for DW.

For SW, the Fano shaped G^- mode is not present while the G^+ mode is upshifted from 1591.5 ± 0.2 to 1603.7 ± 0.4 cm^{-1}. The doping effect is constant within the temperature range explored. For DW, the G^+ mode associated with the outer nanotube is upshifted by 18 ± 0.4 cm^{-1} due to doping, while the G^+ mode associated to the inner nanotube is upshifted by only 3.2 ± 0.8 cm^{-1}. The Raman spectra have been fitted using two Lorentzian line shapes. The differences observed for inner and outer nanotubes gives a direct measure of the strain-induced shifts experienced by the inner nanotube and dynamical effects and strain-induced shift on the outer nanotube. A slight decrease in wave number of the G^+ bands is observed when increasing the temperature, which can be explained by anharmonic effects.

B. High pressure: DW

The relation between the tangential strain due to pressure of inner and outer nanotubes has been established earlier and

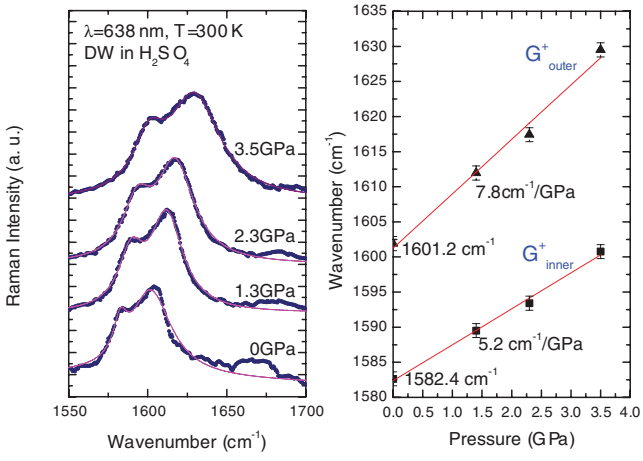

FIG. 2. (Color online) High pressure on DW using H_2SO_4 as the pressure-transmitting medium. The G^+ bands of inner and outer nanotubes are well resolved at zero pressure.

TABLE I. Raman shifts at zero pressure as a function of doping for DW. Argon as the pressure-transmitting medium is used as a reference. The DW samples used in the two experiments come from different sample batches.

Medium	$\Delta\omega_i$ (cm^{-1})	$\Delta\omega_o$ (cm^{-1})
H_2SO_4 from Ref. 17	6 ± 0.5	26 ± 0.5
H_2SO_4	1.4 ± 0.5	9.3 ± 0.5

is well defined.[18] Using argon as the pressure-transmitting medium, the G^+-band shift of the outer nanotube is 1.7 times larger than the G^+-band shift of the inner nanotube.[36] We have used highly concentrated sulfuric acid earlier and found the zero-pressure values for the phonon wave number.[17] In Fig. 2, the value found for both inner (i) and outer (o) nanotubes are $\omega_{G+o} = 1601.2 \pm 0.8$ cm^{-1}, $d\omega_{G+o}/dP = 7.8 \pm 0.6$ cm^{-1}, $\omega_{G+i} = 1582.4 \pm 0.4$ cm^{-1}, and $d\omega_{G+i}/dP = 5.2 \pm 0.3$ cm^{-1}. The ratio $\Delta\omega_o/\Delta\omega_i$ is 1.5 ± 0.2. The Table I lists the measured values. As the samples come from different sample batches, a small change of the DW mean diameter is probably at the origin of the observed differences.

The quasilinearity of the Raman shift for both G bands as a function of pressure has been established experimentally. The band position is deduced using the fit with two Lorentzians. The ratio of the G^+-band shift of the outer nanotube to G^+-band shift of the inner nanotube is 1.5, which is close to 1.7 obtained when using argon as the pressure-transmitting medium. The band shift of the outer nanotube includes lattice contraction and a contribution from nonadiabatic effects. The ruby lines shift without an increase in half width at half maximum (HWHM). The HWHM stays close to 7 ± 1 cm^{-1}. This shows that hydrostatic pressure conditions are maintained below 10 GPa.

IV. INTERACTION OF SPECIES ON GRAPHENE LAYER USING DFT CALCULATIONS

To explore the effect of chemical doping on the electronic structure, we have carried out DFT calculations. To reduce the complexity due to numerous nanotube chiralities,[37] we have focused our attention on a single graphene layer. These calculations are important first for interpreting GIC-H_2SO_4 systems but also for estimating the effect on nanotubes, neglecting curvature effects, as a first approximation.

DFT calculations have been performed to see how each species in sulfuric acid solution interacts with graphene and how the electronic band structures is modified. Modifications in the electronic band structures change the Fermi velocity v_F and the electron momentum relaxation time τ. The latter results from all possible momentum exchange scattering mechanisms of the electrons near the Fermi surface. A nonadiabatic effect will be present when the two following conditions are satisfied: $|\mathbf{q} \cdot \mathbf{v}_F| \ll \omega$ and $\hbar\omega \gg \sigma$, with $\hbar\omega$ the G phonon energy, q the wave vector, and $\sigma = h/\tau$.[38,39] From the work of Saitta *et al.*, on giant nonadiabatic effects in GIC,[9] we know that a large relaxation time of the electrons near the Fermi surface is a good indicator of nonadiabaticity. Figure 3 shows the electronic band structures of pristine

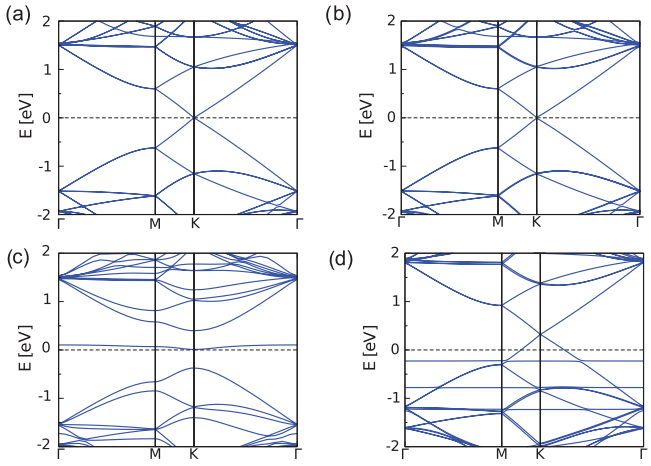

FIG. 3. (Color online) Electronic band structure for a single graphene layer (a) pristine, (b) in contact with H_2SO_4, (c) in contact with a H adatom with a the new state close to the Fermi level, and (d) in contact with HSO_4 with a new state below the Fermi level.

graphene and graphene in interaction with H_2SO_4, H, and HSO_4. For pristine graphene, the conduction and valence bands meet at the K point (the Fermi level is indicated with a dashed line). When a single H_2SO_4 molecule is approaching the graphene surface, it is only physisorbed and thus no charge transfer occurs. This observation is in contradiction with a previous study.[20] However, this difference can be explained by the use of a simple local density approximation of exchange correlation functional in the work of Cordero and Alonso.[20] This approximation is well known to exaggerate artificially the electron density delocalization, leading to a too-large charge transfer between the two. Results from GIC with $C_p{}^+HSO_4{}^- \cdot x(H_2SO_4)$ (charge transfer $f_C = 1/p$)[7] and reversible protonation of SW reported in literature[11,12] show that species H and HSO_4 need to be considered.

It is important to keep in mind that pure H_2SO_4 is more complex as it contains $HSO_4{}^-$, $H_3SO_4{}^+$, H_3O^+, $HS_2O_7{}^-$, $H_2S_2O_7$, and traces of H_2O (Ref. 40). When hydrogen atoms are positioned in the vicinity of the surface, they move closer to the surface forming a quasi-covalent C-H bond. As a consequence, the electronic band structure is strongly affected and a large gap is opening up. The Fermi level is positioned in the middle of the band gap and close to the localized states induced by the presence of hydrogen. In the presence of a positive charge on H, the electronic band structure remains the same and only the position of the Fermi level is modified. The presence of HSO_4 on graphene creates localized electronic states which are far from the Dirac point. Thus, the electronic properties in the latter case are similar to the ones induced by a gate voltage. We have also observed that the charge transfer leads to charge configuration close to the one of $HSO_4{}^-$ and $C_p{}^+$. The Fermi level is consequently shifted to the valence band and indicates a strong p doping. When placing a single H adatom and an HSO_4 molecule close to a graphene layer, we find that they spontaneously reform the H_2SO_4 molecule. Additionally, no spontaneous dissociation of H_2SO_4 was found on a pristine surface. This implies that only a limited number of ions are in contact with the surface.

In summary, we have explored several molecular species interacting with graphene. We find some of them modify the Fermi level without significant modification of the electronic band structure at the Fermi level and hence contribute to the change of the phonon energy via nonadiabatic effects. This is the case for $HSO_4{}^-$. Other molecules like H^+ lead to a charge transfer and modify the electronic band structure of pristine graphene. In this case, a full calculation is needed to know how the phonon energy is modified, which is challenging for acid solutions. We expect fewer nonadiabatic effects due to electronic band structure distortion in the presence of H^+. Finally, we find that some molecules such as H_2SO_4 do not participate in transfer of holes or electrons and do not contribute to the dynamical effect.

V. DISCUSSION

A. GIC-H_2SO_4

In Fig. 4(a), the experimental values of the G-band wave number of the GIC-H_2SO_4 stage one and two compounds are plotted as a function of charge transfer per carbon atom. The function which fits the two points consists of a linear and a square-root term. The linear term due to strain $\Delta\omega_s$ (cm^{-1}) = 350 f_C is consistent with neutron measurements and DFT calculation[8] and has been kept fixed. It is assumed that the doping effect is isotropic. When fitting, we only varied the prefactor of the square-root term. The prefactor for $\sqrt{f_C}$ is 204 ± 8, which is close to the value found from first-principles calculations using a gate voltage.[8] The linear strain shift is deduced using the lattice parameter variation as determined

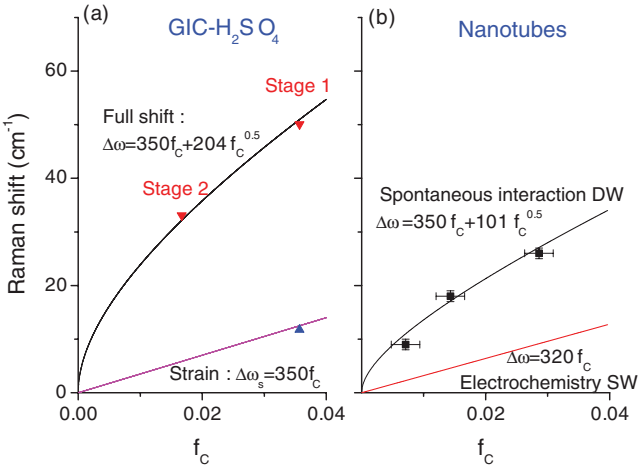

FIG. 4. (Color online) (a) G mode shift versus the charge transfer for GIC-H_2SO_4 (red upper triangles) with fitted line using a fixed linear term and an adjustable prefactor for the square root term (black line). The lattice contractions were extracted from neutron data (blue lower triangle) (Ref. 19) and converted to Raman shifts using high-pressure data (Ref. 41). The linear term (purple line) has been obtained from DFT calculation (Ref. 8). (b) Raman shift of the outer nanotube of DW with f_C deduced from Raman G^+-band shift of the inner nanotube (black squares) and fitted line using a fixed linear term and an adjustable prefactor for the square root term (black line). The Raman shift deduced from electrochemical data is also reported (red line) (Ref. 4). The same scale has been used for all plots.

by neutron diffraction ($da/a = 0.0025$)[19] and the G-band shift as a function of pressure of graphite ($da/a = 2.1 \times 10^{-4} d\omega$).[41] We note that there is a difference of -20 cm^{-1} in the slope between the DFT calculations and the experimental strain-induced shifts. This small error in the slope demonstrates that the bond contractions due to charge transfer are consistent with the bond contractions measured by applying a hydrostatic pressure.

In GIC, H_2 is partially removed during electrochemical intercalation and the main interacting species with graphene is HSO_4^-. From Fig. 3, it is seen that the additional state introduced with HSO_4^- is far from the Fermi level and the charge transfer is similar to what has been found when using a gate voltage. The electronic band structure is assumed to be affected only to a minor degree, leading to a large nonadiabatic effect. Our DFT calculation shows that HSO_4^- is a dopant which does not alter the electronic band structure in an important way.

B. Nanotubes with H_2SO_4

The spontaneous interaction of sulfuric acid with nanotubes is different, however. H^+ ions are still present and not removed, as in the case of intercalating. In Fig. 4(b) we have plotted the linear shift $\Delta\omega$ (cm^{-1}) $= 320 f_C$ of Sumanasekera *et al.*[4] obtained by charging SW after a first spontaneous interaction. The slope is very close to what has been found for the experimental strain shift found in Fig. 4(a). So far it is not clear why nonadiabatic effects are not observed here.

Figure 4(b) shows the effect of chemical doping on DW. The shift of the inner nanotube is taken as a reference for strain. The strain on the inner nanotube is reduced due to the presence of the outer nanotube and one can obtain the strain on the outer nanotube by multiplying the measured strain of the inner nanotube by 1.7. This value has been observed experimentally[17] and also determined by model calculations.[18] We can convert the strain shift to charge transfer using the conversion factor as deduced from DFT calculation: $\Delta\omega_s = 350 f_C$. The resulting values are plotted in Fig. 4(b) for DW. The dependence with charge transfer per carbon atom is nonlinear, indicating clearly that a nonadiabatic effect is observed for nanotubes. We again fit the points with a linear and a square-root term and obtain $\Delta\omega$ (cm^{-1}) $= (350 \pm 20) f_C + (101 \pm 8)\sqrt{f_C}$. As before, only the prefactor of the square root term has been fitted. The prefactor is lower by a factor of about two compared to GIC-H_2SO_4.

We clearly see here the difference between SW by electrical charging using an applying field after a first spontaneous interaction and DW without any applied field after a first spontaneous interaction. The experimental conditions are not equivalent. By applying a field, the CNTs can be positively charged and the Raman shift of the G band is not associated with the strength of the sulfuric acid solutions but only on the local charge equilibrium. The Raman shift found is in this case linear. When no field is applied, however, there is the spontaneous interaction of CNTs with sulfuric acid solutions and the Raman shift depends on the concentration of the sulfuric acid.

To explain the difference of the prefactor we note that in the case of GIC, we have shown that there is only one type of dominant HSO_4^- ion in interaction with the graphene layer. The Fermi level is shifted without modifying the electronic band structure. The nanotubes in sulfuric acid, however, are interacting with two dominant species H^+ (and associated species) and HSO_4^-. From Fig. 3, one can see that H^+ ions change strongly the electronic band structure affecting the phonon shift, but only a smaller nonadiabatic effect is expected. The effect of H^+ ions is difficult to fully access since the surrounding medium needs to be included in the calculation. The nanotubes in sulfuric acid are influenced by one species (HSO_4^-) which induced nonadiabatic effects and one species (H^+) which induced only a small nonadiabatic effect. The two situations for GIC and the nanotubes are therefore very different, which is reflected in the difference of the prefactor in front of the square-root term. Our determination of the Raman shift versus hole charge transfer thus *measures the spontaneous interaction* between the sulfuric acid and the nanotube. It is important to keep in mind that only the main species have been considered here and other species are expected to contribute to a minor degree to the observed spectral shift.

VI. CONCLUSION

We considered the spontaneous interaction of sulfuric acid as a function of concentration and temperature with CNTs using the Raman G band. The results are compared with intercalated graphite. In order to separate strain and nonadiabatic effects due to charge transfer on the phonon energy, we have used DW. The inner nanotube is used as a strain indicator. This allowed us to identify two effects to the observed Raman G-band shift associated to the outer nanotube. The total shift is found to be $\Delta\omega$ (cm^{-1}) $= (350 \pm 20) f_C + (101 \pm 8)\sqrt{f_C}$ when using sulfuric acid solutions. By using the relation from Sumanasekera *et al.*,[4] we are overestimating the nanotube charging. DFT calculations exploring the interaction of ions on the band structure of graphene showed that HSO_4^- keeps the electronic band structure intact but leads to a large nonadiabatic effect, while H^+ modifies the electronic band structure and leads to only a small nonadiabatic effect. While doping of CNT is always associated with protonation, we have shown that HSO_4^- plays an important role and needs to be fully taken into account to explain the observed phonon shifts to detect accurately charge transfer on CNT.

*pascal.puech@cemes.fr

[1] Y. Zhao, J. Wei, R. Vajtai, P. M. Ajayan, and E. V. Barrera, Nat. Sci. Rep. **83**, (2011).

[2] L. M. Ericson *et al.*, Science **305**, 1447 (2004).

[3] V. A. Davis, A. N. G. Parra-Vasquez, M. J. Green, P. K. Rai, N. Behabtu, V. Prieto, R. D. Booker, J. Schmidt, E. Kesselman, W. Zhou, H. Fan, W. Wade Adams, R. H. Hauge, J. E. Fischer, Y. Cohen, Y. Talmon, R. E. Smalley, and M. Pasquali, Nat. Nanotechnol. **4**, 830 (2009).

[4] G. U. Sumanasekera, J. L. Allen, S. L. Fang, A. L. Loper, A. M. Rao, and P. C. Eklund, J. Phys. Chem. B **103**, 4292 (1999).

[5]L. Kavan and L. Dunsch, Chem. Phys. Chem. **8**, 974 (2007).
[6]T. Hu and I. Gerber (unpublished).
[7]P. C. Eklund, C. H. Olk, F. J. Holler, J. G. Spolar, and E. G. Arakawa, J. Mater. Res. **1**, 361 (1986).
[8]M. Lazzeri and F. Mauri, Phys. Rev. Lett. **97**, 266407 (2006).
[9]A. M. Saitta, M. Lazzeri, M. Calandra, and F. Mauri, Phys. Rev. Lett. **100**, 226401 (2008).
[10]S. Ramesh, L. M. Ericson, V. A. Davis, R. K. Saini, C. Kittrell, M. Pasquali, W. E. Billups, W. W. Adams, R. H. Hauge, and R. E. Smalley, J. Phys. Chem. B **108**, 8794 (2004).
[11]W. Zhou, P. A. Heiney, H. Fan, R. E. Smalley, and J. E. Fisher, J. Am. Chem. Soc. **127**, 1640 (2005).
[12]C. Engtrakul, M. F. Davis, T. Gennett, A. C. Dillon, K. M. Jones, and M. J. Heben, J. Am. Chem. Soc. **127**, 17548 (2005).
[13]W. Zhou, J. E. Fischer, P. A. Heiney, H. Fan, V. A. Davis, M. Pasquali, and R. E. Smalley, Phys. Rev. B **72**, 045440 (2005).
[14]M. S. Strano, C. B. Huffman, V. C. Moore, M. J. O'Connell, E. H. Haroz, J. Hubbard, M. Miller, K. Rialon, C. Kittrell, S. Ramesh, R. H. Hauge, and R. E. Smalley, J. Phys. Chem. B **107**, 6979 (2003).
[15]S. Reich, C. Thomsen, and J. Maultzsch, *Carbon Nanotubes: Basic Concepts and Physical Properties* (Wiley-Verlag, Berlin, 2004).
[16]E. B. Barros, H. Son, Ge. G. Samsonidze, A. G. Souza Filho, R. Saito, Y. A. Kim, H. Muramatsu, T. Hayashi, M. Endo, J. Kong, and M. S. Dresselhaus, Phys. Rev. B **76**, 045425 (2007).
[17]P. Puech, A. Ghandour, A. Sapelkin, C. Tinguely, E. Flahaut, D. J. Dunstan, and W. Bacsa, Phys. Rev. B **78**, 045413 (2008).
[18]P. Puech, H. Hubel, D. Dunstan, R. R. Bacsa, C. Laurent, and W. S. Bacsa, Phys. Rev. Lett. **93**, 095506 (2004).
[19]C. T. Chan, W. A. Kamitakahara, K. M. Ho, and P. C. Eklund, Phys. Rev. Lett. **58**, 1528 (1987).
[20]N. A. Cordero and J. A. Alonso, Nanotechnology **18**, 485705 (2007).
[21]E. Flahaut, R. Bacsa, A. Peigney, and Ch. Laurent, Chem. Commun. **12**, 1442 (2003).
[22]G. J. Piermari, S. Block, and J. D. Barnett, J. Appl. Phys. **44**, 5377 (1973).
[23]D. C. Montgomery, E. A. Peck, and G. G. Vining, *Introduction to Linear Regression Analysis*, 4th ed. (Wiley-Interscience, New York, 2006).
[24]G. Kresse and J. Hafner, Phys. Rev. B **47**, 558 (1993).
[25]G. Kresse and J. Hafner, Phys. Rev. B **49**, 14251 (1994).
[26]G. Kresse and J. Furthmüller, Comput. Mater. Sci. **6**, 15 (1996).
[27]G. Kresse and J. Furthmüller, Phys. Rev. B **54**, 11169 (1996).
[28]P. E. Blochl, Phys. Rev. B **50**, 17953 (1994).
[29]G. Kresse and D. Joubert, Phys. Rev. B **59**, 1758 (1999).
[30]J. P. Perdew, K. Burke, and M. Ernzerhof, Phys. Rev. Lett. **77**, 3865 (1996).
[31]H. Rydberg, M. Dion, N. Jacobson, E. Schröder, P. Hyldgaard, S. I. Simak, D. C. Langreth, and B. I. Lundqvist, Phys. Rev. Lett. **91**, 126402 (2003).
[32]A. Gulans, M. J. Puska, and R. M. Nieminen, Phys. Rev. B **79**, 201105 (2009).
[33]W. Tang, E. Sanville, and G. Henkelman, J. Phys.: Condens. Matter **21**, 084204 (2009).
[34]E. Sanville, S. D. Kenny, R. Smith, and G. Henkelman, J. Comput. Chem. **28**, 899 (2007).
[35]G. Henkelman, A. Arnaldsson, and H. Jónsson, Comput. Mater. Sci. **36**, 254 (2006).
[36]P. Puech, E. Flahaut, A. Sapelkin, H. Hubel, D. J. Dunstan, G. Landa, and W. S. Bacsa, Phys. Rev. B **73**, 233408 (2006).
[37]N. Caudal, A. M. Saitta, M. Lazzeri, and F. Mauri, Phys. Rev. B **75**, 115423 (2007).
[38]S. Engelsberg and J. R. Schieffer, Phys. Rev. **131**, 993 (1963).
[39]E. G. Maksimov and S. V. Shulga, Solid State Commun. **97**, 553 (1996).
[40]N. Greenwood and A. Earnshaw, *Chemistry of the Elements*, 2nd ed. (Butterworth-Heinemann, Oxford, 1997).
[41]M. Hanfland, H. Beister, and K. Syassen, Phys. Rev. B **39**, 12598 (1989).